ELSEVIER

Journal of Hazardous Materials 53 (1997) 35–55

JOURNAL OF HAZARDOUS MATERIALS

# Development of a model to predict the effects of explosions in compact congested regions

R.P. Cleaver *, C.E. Humphreys, J.D. Morgan, C.G. Robinson

*British Gas plc, Research and Technology, Gas Research Centre, Ashby Road, Loughborough, Leicestershire LE11 3QU, UK*

Received 30 March 1996; accepted 6 May 1996

**Abstract**

In this paper it is shown how a number of models can be produced and linked together to predict the consequences of a vapour cloud explosion in a compact region of congestion on a typical gas processing or storage site. The individual models address the generation of pressure within the congested region, the propagation of the resulting pressure wave away from the region and the load received by any obstacle on the site outside of the congested region. The performance of each of the models is illustrated and discussed, including comparisons with experimental data. Finally, the application of the models to practical cases is considered. © 1997 Published by Elsevier Science B.V.

*Keywords:* Vapour cloud explosions; Overpressure; Safety; Major hazards

## 1. Introduction

There have been a number of cases in which vapour cloud explosions have occurred on industrial plants. The resulting destruction and loss of life have focused attention on understanding how such explosions occur. As a result of case studies and further experimental and theoretical work, the mechanisms leading to the development of significant pressures have been explained in a qualitative manner. However, to be able to help improve design of future plant, or characterize the extent of the hazard on

* Corresponding author.


*PII* S0304-3894(96)01817-1

existing plant, there is a need for more reliable quantitative methods of assessing the consequences of vapour cloud explosions.

This paper presents one particular approach to providing a method for calculating the consequences of such explosions. The aim is to produce a series of linked models of comparable levels of complexity and accuracy that allow an assessment of the consequences of the effects of the explosion to be made. The models presented here are all of the phenomenological type. They can all be run on a personal computer, with short run times.

The case in which an otherwise unconfined vapour cloud envelopes a compact region of congestion is considered. In this context, the use of the term "compact" refers to a single congested region whose dimensions are approximately equal (near unity aspect ratio). It is necessary to differentiate this type of region from the more elongated, piperack structures found on many sites. For central ignition of a compact region, until the flame first reaches the edge of the region, spherical symmetry may be assumed, thereby allowing the development of a simple type of model. For regions with larger aspect ratios, such as piperacks, this may no longer be the case and it may be necessary to adopt a different approach.

A calculation is carried out to determine the pressure that is generated by the combustion of the vapour cloud. A method of calculating the propagation of the resulting pressure wave away from the source region is then applied and this information is used to estimate the loading received by other structures on the site outside of the congested region. These structures act as obstacles to the propagation of the wave. It is assumed that the time scale for the pressure wave is so short that the loading is unaffected by the slower response of the obstacles. In this way the complex events in an explosion have been divided into a number of separate problems, and it has been assumed that these can be tackled individually.

The first in the sequence of models, the pressure source model, is outlined in Section 2. It is shown in Section 3 that existing formulae for wave propagation can be applied to predict how the resulting pressure wave decays with distance from the source of the explosion. The way in which this time dependent information is then used in predicting the loading received by adjacent obstacles, such as control buildings or storage tanks, is described briefly in Section 4. In each of these sections, the performance of the models is illustrated by comparison with specific experimental data. Finally in Section 5, this approach of using separate, but linked, individual models is discussed. In particular, consideration is given as to how this combination of models could be used in practice.

## 2. Model for the source pressure

### 2.1. Model formulation

In a previous paper [1], a mathematical model was produced to explain the generation of pressure in a congested region produced by a spherically symmetric vapour cloud explosion. The model related the pressure $P(R_f)$ at the mean position of the flame front

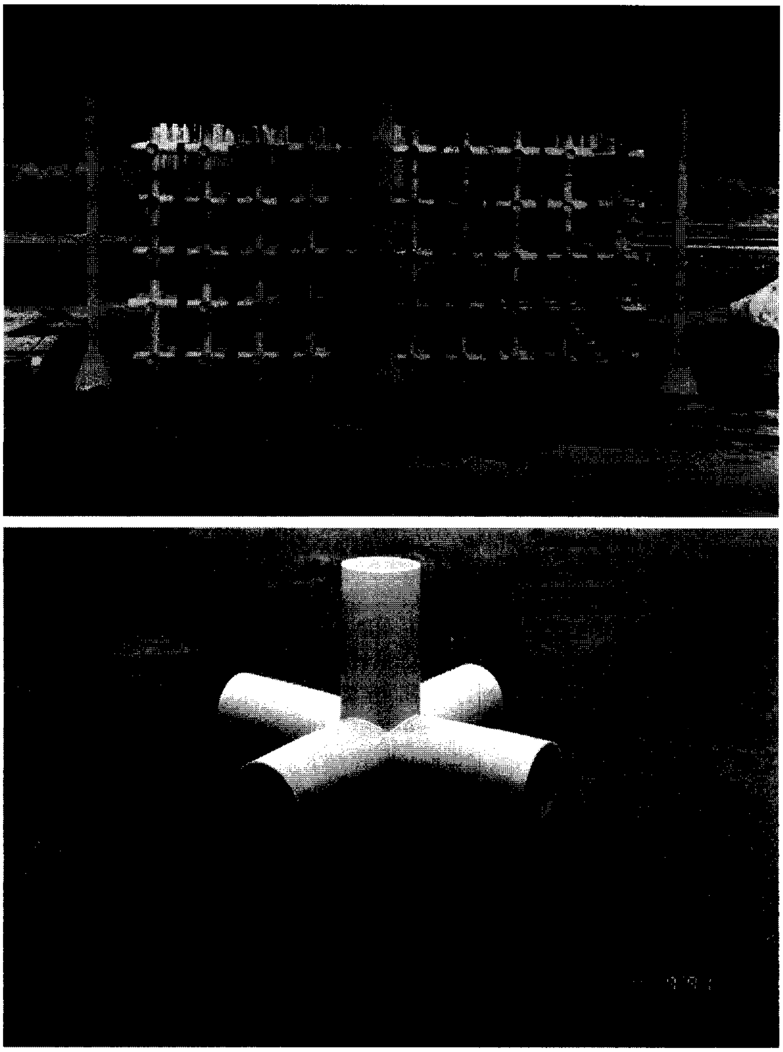

Fig. 1. Illustration of the rig used in the British Gas MERGE experiments. (a) Overall dimensions of the rig and location of the ignition position; (b) one element of the obstacle array.

$R_f$ to the speed $S_f$ and acceleration of the flame and the degree of obstruction ahead of the flame. It was shown that the pressure is given by an expression

$$\frac{P(R_f)}{P_\infty} = \left( \frac{\gamma - 1}{a^2}(A + B - C + D) + 1 \right)^{\gamma/\gamma - 1} \quad (1)$$

where $\gamma$ denotes the ratio of specific heats of the fuel–air mixture ahead of the flame, $a$ the speed of sound in the ambient fluid, given by the equation,

$$a^2 = \frac{\gamma P_\infty}{\rho_\infty}$$

$P_\infty$ denotes the pressure in the ambient fluid, $\rho_\infty$ the density in the ambient fluid and the terms $A$, $B$, $C$ and $D$ are given by the following equations

$$A=\frac{E-1}{E}\left(2S_f^2+R_f\frac{dS_f}{dt}\right)$$

$$B=k_1\left(1-\frac{R_f}{R_c}\right)A$$

$$C=\frac{1}{2}\left(S_f\frac{E-1}{E}\right)^2$$

and

$$D=k_2\frac{R_f}{3}\left(1-\left(\frac{R_f}{R_c}\right)^3\right)C$$

In the above equations, $S_f=(dR_f/dt)$, $t$ is the time, $E$ is the expansion ratio of the fuel–air mixture, $R_c$ is the radius of an equivalent spherical volume representing the congested region and $k_1$ and $k_2$ are constants associated with the inertial and form drag exerted on the fluid by the obstacles inside the congested region [1].

The applicability of this model was demonstrated for the data collected by British Gas as part of EU funded project MERGE. In the experiments, a congested array in the form of half of a cube was constructed and positioned at ground level as shown in Fig. 1(a). The array was made up from individual nodes of the type shown in Fig. 1(b). The nodes were connected by spacer bars of the same diameter and length, with the result that the pitch between successive rows of obstacles was the same in each of the three perpendicular directions. The enclosure was surrounded by polythene sheeting that was kept rigidly in place at the edges. It was filled with stoichiometric mixtures of various fuel gases and air. After sufficient time had elapsed to ensure that the mixtures were

Table 1
Parameters describing the experimental rigs used in the EU sponsored projects MERGE and EMERGE

| Rig type | Pipe | | Volume blockage (%) | Dimensions of the congested region (m) |
|---|---|---|---|---|
| | Diameter (mm) | Spacing (mm) | | |
| A | 43 | 200 | 10 | 4.0×4.0×2.0 |
| B | 41 | 133 | 20 | 4.0×4.0×2.0 [a] |
| C | 86 | 400 | 10 | 4.0×4.0×2.0 |
| D | 82 | 267 | 20 | 4.3×4.3×2.1 |
| E | 168 | 800 | 10 | 8.0×8.0×4.0 |
| C* | 82 | 384 | 10 | 7.6×7.6×3.7 |
| F | 43 | 283 | 5 | 4.0×4.0×2.0 [b] |

[a] For the propane test this was reduced to 3.5×3.5×1.7 due to the high pressure obtained in the methane/propane test.
[b] This rig was not used in project MERGE, but was used in project EMERGE.

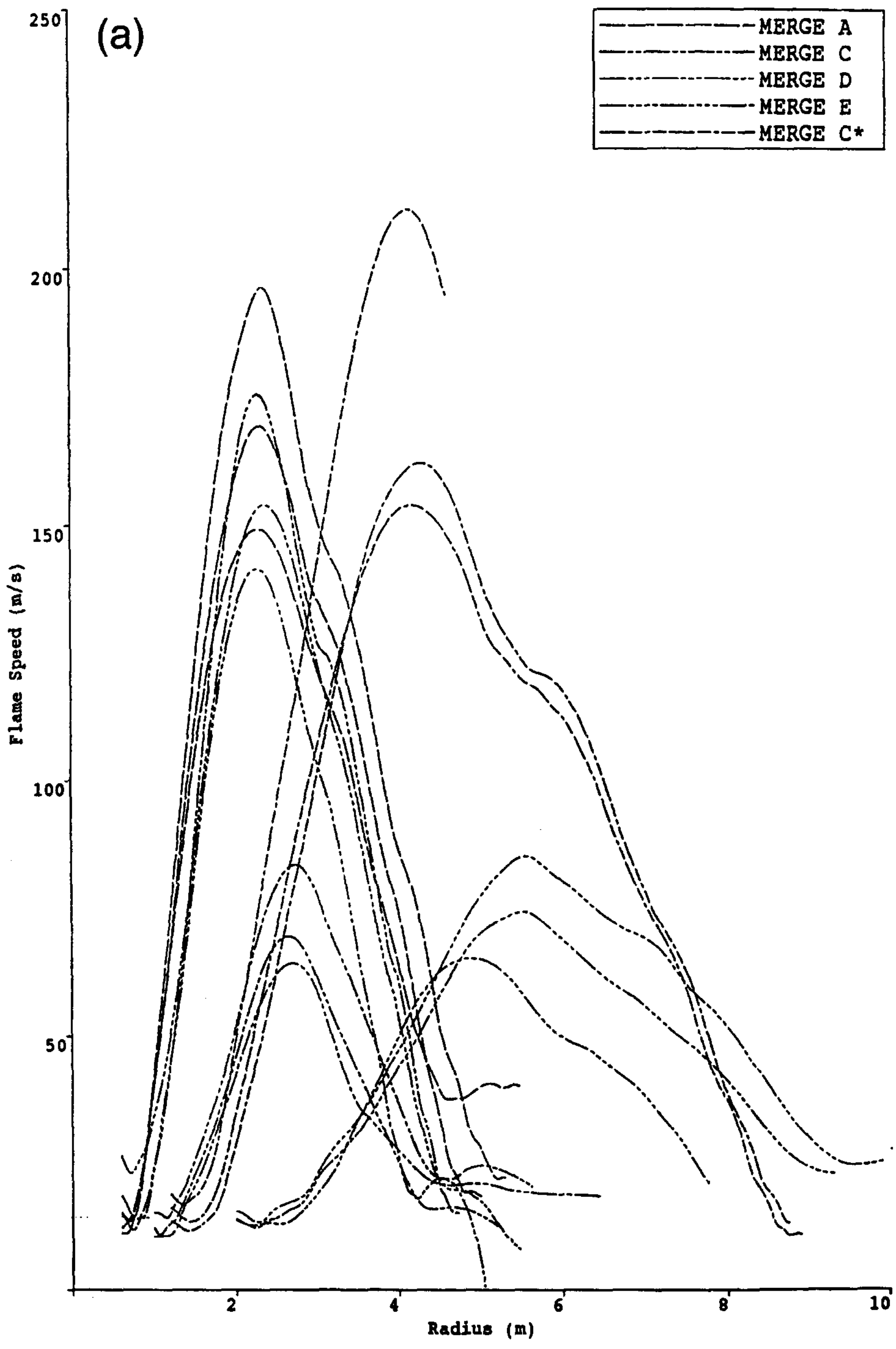
(a)
MERGE A
MERGE C
MERGE D
MERGE E
MERGE C*
250
200
150
100
50
Flame Speed (m/s)
2
4
6
8
10
Radius (m)

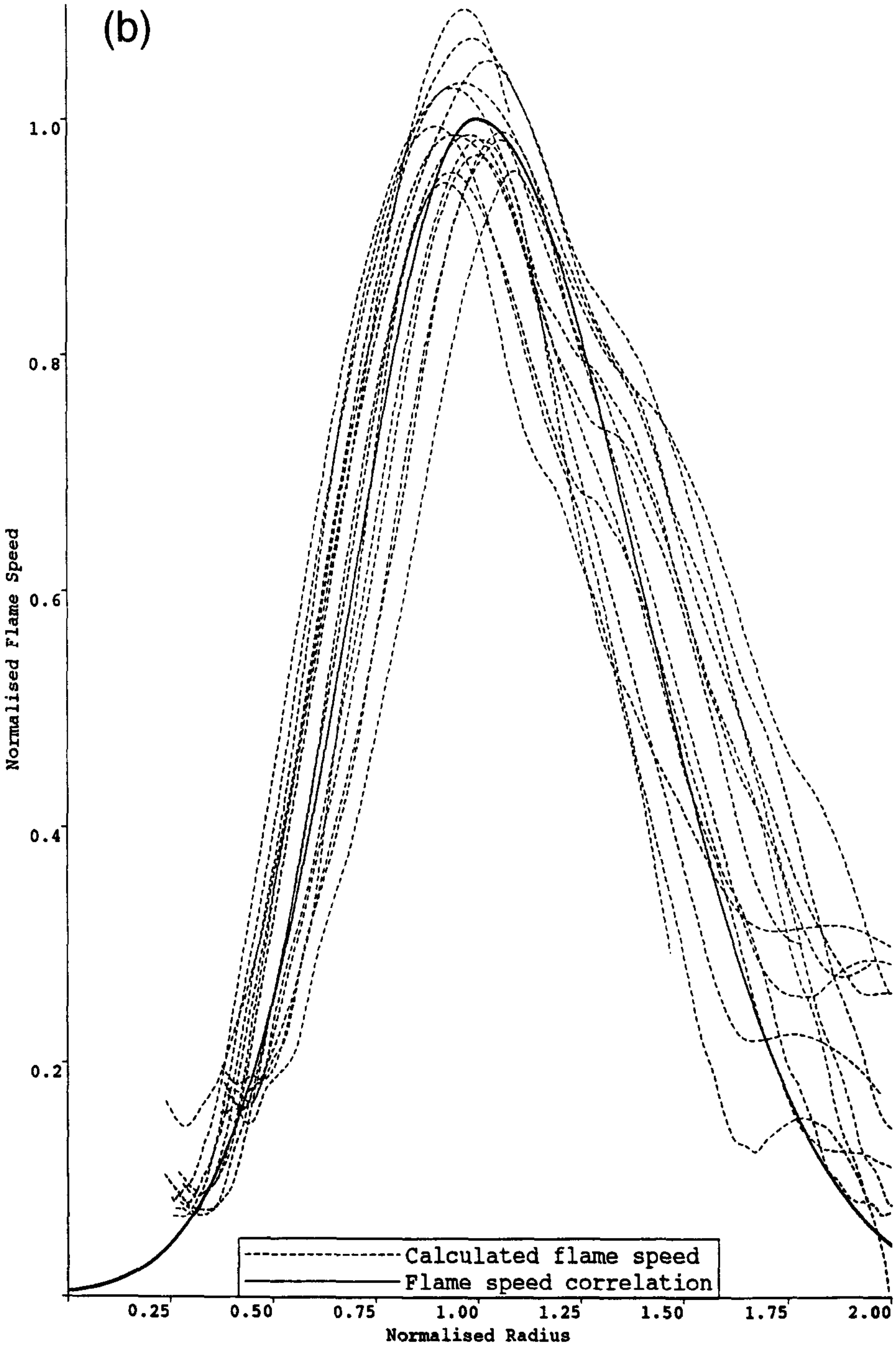
(b)
Normalised Flame Speed
1.0
0.8
0.6
0.4
0.2
0.25
0.50
0.75
1.00
1.25
1.50
1.75
2.00
Normalised Radius
Calculated flame speed
Flame speed correlation

quiescent, the gas–air mixture was ignited by a single, low energy spark. The ignition position was as close as possible to the middle of the square whose sides are defined by the lines of intersection between the vertical planes defining the boundaries of the array and the ground plane. Prior to the ignition of the mixture, the polythene sheet covering the rig was cut by low energy detonating chord. Different combinations of pipe diameter and pipe spacing were investigated during the experimental programme and tests were carried out at two different size of rig. Table 1 gives details of the range of parameters studied and introduces the lettering scheme used to denote each different configuration. An overview of project MERGE, including further details of these experiments, is given by Mercx [2].

Fig. 2(a) shows the results of applying the model described above to predict the mean flame speed as a function of distance from the ignition position for the different experimental configurations. The values for the flame speed were obtained by integrating the measured values for the pressure, as described in [1]. The flame speeds and pressures generated in the MERGE series B experiments were so large that compressibility effects become important and the mathematical model outlined in [1] is not applicable. However, it was observed that the remaining values could be made to overlay each other approximately if they were normalized using the maximum value of the flame speed $S_{f_{max}}$ and an appropriate length scale, $L$. This is illustrated in Fig. 2(b). Also shown on this figure is a single solid curve that passes approximately through the middle of the various individual, normalized flame speed curves. This curve is described by an equation in the form:

$$S_f = S_{f_{max}} e^{-\left(\frac{1}{2}\left(\frac{R_f - L}{\sigma L}\right)^2\right)} \qquad (2)$$

where

$$\sigma = 0.3 \text{ for } \frac{R_f}{L} \leq 1$$

and

$$\sigma = 0.4 \text{ for } \frac{R_f}{L} > 1$$

To make use of this common trend in the data over the range of experiments that have been studied, correlations have been produced defining $S_{f_{max}}$ and $L$ in terms of the parameters that describe the geometry and the fuel. The geometric parameters that have been used are the average volume blockage and the average pipe diameter within the congested region and the size of the region. The fuel dependency is introduced through the laminar burning velocity of the gas–air mixture.

The correlation, Eq. (2), for the flame history can then be used with the mathematical

Fig. 2. Flame speeds deduced from the overpressure measurements for the experiments conducted by British Gas as part of the MERGE programme. The letters denote the different rigs used in the experiments, as defined in Table 1. In (a) the speeds in m s$^{-1}$ are plotted against distance in m, whereas in (b) they are shown in a normalized form, together with the curve fit used in the mathematical model.

equation, Eq. (1), to define a value for the pressure at, and also by assumption behind, the flame. That is, the combination of the correlations and the mathematical relationships produce a predictive model for the source pressure as a function of time for the case of the central ignition of a vapour cloud occupying a compact, congested region, provided suitable values can be defined for the geometric parameters. For the idealized type of experiment in the MERGE project, the geometric parameters are defined unambiguously, as shown in Table 1, and the assumptions used in the mathematical model of a spherically symmetric flow field ahead of the flame appear to be valid. The application of the method to a realistic geometry, containing a distribution of pipe sizes, is discussed further in Section 5.

The effects that are produced by initial turbulence in the neighbourhood of the ignition point can be modelled using the same approach. Experiments were carried out by British Gas as part of a second EU funded project, EMERGE, to investigate the effects such initial turbulence produces. The data collected during the experiments in which a turbulence field was present prior to ignition has been analysed using the approach in [1]. This has shown that a small region of turbulence surrounding the ignition position produces a perturbation to the flame speed at early times. A correlation has been produced to describe this, with the magnitude of the perturbation dependent on the initial root-mean-square turbulence velocity and the length-scale of the turbulence in this region. This perturbation can then be added to the expression Eq. (2) to define a flame speed for this case. It is then assumed that the same mathematical model can be used as in the initially quiescent cases to predict the resulting pressures.

### 2.2. Model comparison

The model was first applied to predict the overpressures for the various MERGE experiments used in the derivation of the correlation. The results are illustrated in Fig. 3. In this, and later figures, the solid line denotes the experimentally measured overpressure and the dashed line the value predicted by the model. As data from these experiments had been used to deduce the correlation given in Eq. (2), the good agreement between the resulting observed and predicted overpressures provides only limited confirmation of the validity of the model. However, the model has been used to make predictions for the experiments that formed part of the subsequent EMERGE test series. In one test rig, identified by the letter F, the volume blockage was approximately 5% and the diameter of the obstacles was 43 mm (see Table 1). In project MERGE, volume blockages of 10 and 20% were studied. Hence, in terms of the degree of confinement, this set of conditions represents an extrapolation outside the range used in project MERGE. A comparison of the predicted overpressures with the overpressures measured in this EMERGE experiment are shown in Fig. 4(a) for an initially quiescent vapour cloud containing natural gas and in Fig. 4(b) for propane. Both in terms of the timing and shape of the overpressures, the results are encouraging.

The model has also been compared with data from the EMERGE experiments in which there was an initial region of turbulence surrounding the ignition position. The overpressures that are predicted in the cases of a high level of initial turbulence (turbulent rms velocity approximately $12\,\mathrm{m\,s^{-1}}$) and a low level of turbulence (rms

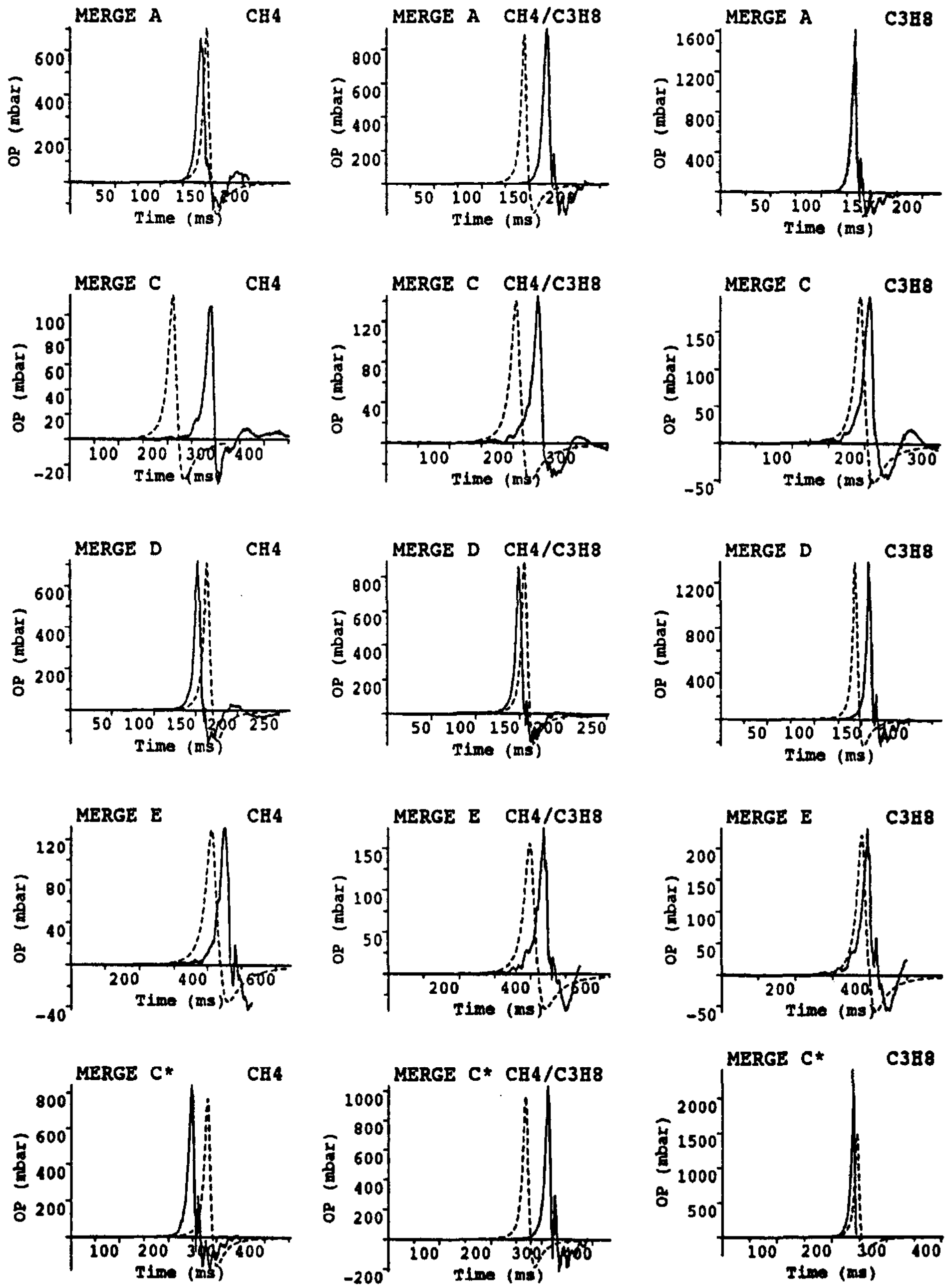


Fig. 3. Comparison of the predicted overpressures, shown by the dotted lines, with the observed overpressures, shown by the solid line, for the experiments conducted as part of the MERGE programme.

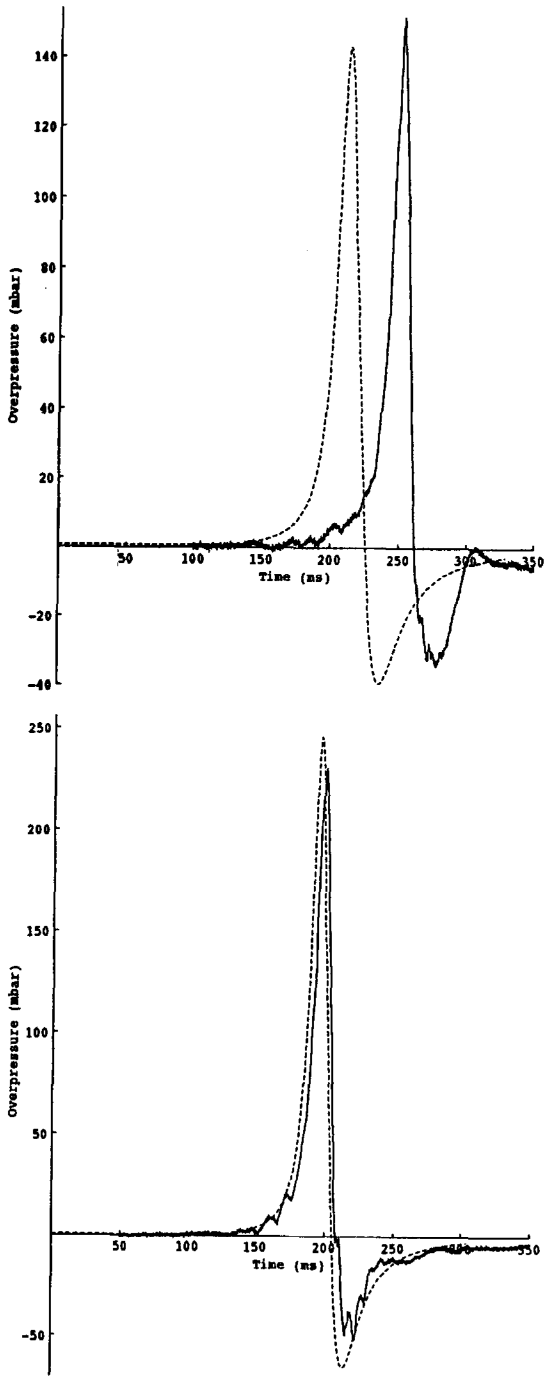
Overpressure (mbar)
140
120
100
80
60
40
20
-20
-40
50
100
150
200
250
300
350
Time (ms)
Overpressure (mbar)
250
200
150
100
50
-50
50
100
150
200
250
300
350
Time (ms)

velocity approximately 1.2 m $s^{-1}$) within the rigs denoted by letters A and F are compared with the experimental results in Fig. 5. The resulting perturbation to the overpressure history at early times is illustrated in greater detail in Fig. 6. Individual graph titles describe the fuel and turbulence level. This shows that in this particular case, in which the initial turbulence occupies a small fraction of the overall congested region, only local perturbations in pressure are produced at early times. Further, the extent of the perturbation is reproduced by the mathematical model.

It should be noted that this method uses ''averaged'' geometric parameters to predict an ''average'' pressure behind the flame. Further, the correlation used in the model is for the average position of the flame within the congested region. The model does not give predictions for the detailed processes that are occurring when the combustion zone interacts with individual obstacles. It would require a more sophisticated approach, such as a computational fluid dynamic code, to explore the behaviour at that level of detail.

## 3. Pressure wave propagation model

### 3.1. Model formulation

One particular feature of the model discussed above is that it predicts the time dependence of an explosion. This information can be used to define the initial conditions for methods of predicting the propagation of the pressure wave into free space. Van den Berg [3] studied how this takes place using a computational fluid dynamic code to solve the governing fluid flow equations for the particular case of a spherically symmetric flame propagating at a specified rate through a given source volume. The results of the calculations were subsequently used within the correlations in the TNO multi-energy methodology. Puttock [4] has shown that simple correlations can also be used to describe numerical solutions for the propagation of the type of waveforms generated in the MERGE test programme and he demonstrated that this approach correctly reproduces the behaviour observed in the MERGE tests carried out by British Gas. Puttock argued further that these correlations can be used as the basis of a method describing the propagation of general overpressure waves. In the work described here, an alternative approach is taken and a series of approximate equations are used to predict the advancement of the waveform.

The method is based on the assumption that the advance of a general pressure wave can be determined from the relationships used to describe the propagation of a shock wave in still air. That is, it is assumed that the speed of propagation, $w$, of each point on

Fig. 4. Comparison of the observed and predicted overpressures for two particular tests in the EMERGE programme: (a) natural gas test; (b) propane test. Both tests have an initially quiescent mixture (zero initial turbulence).

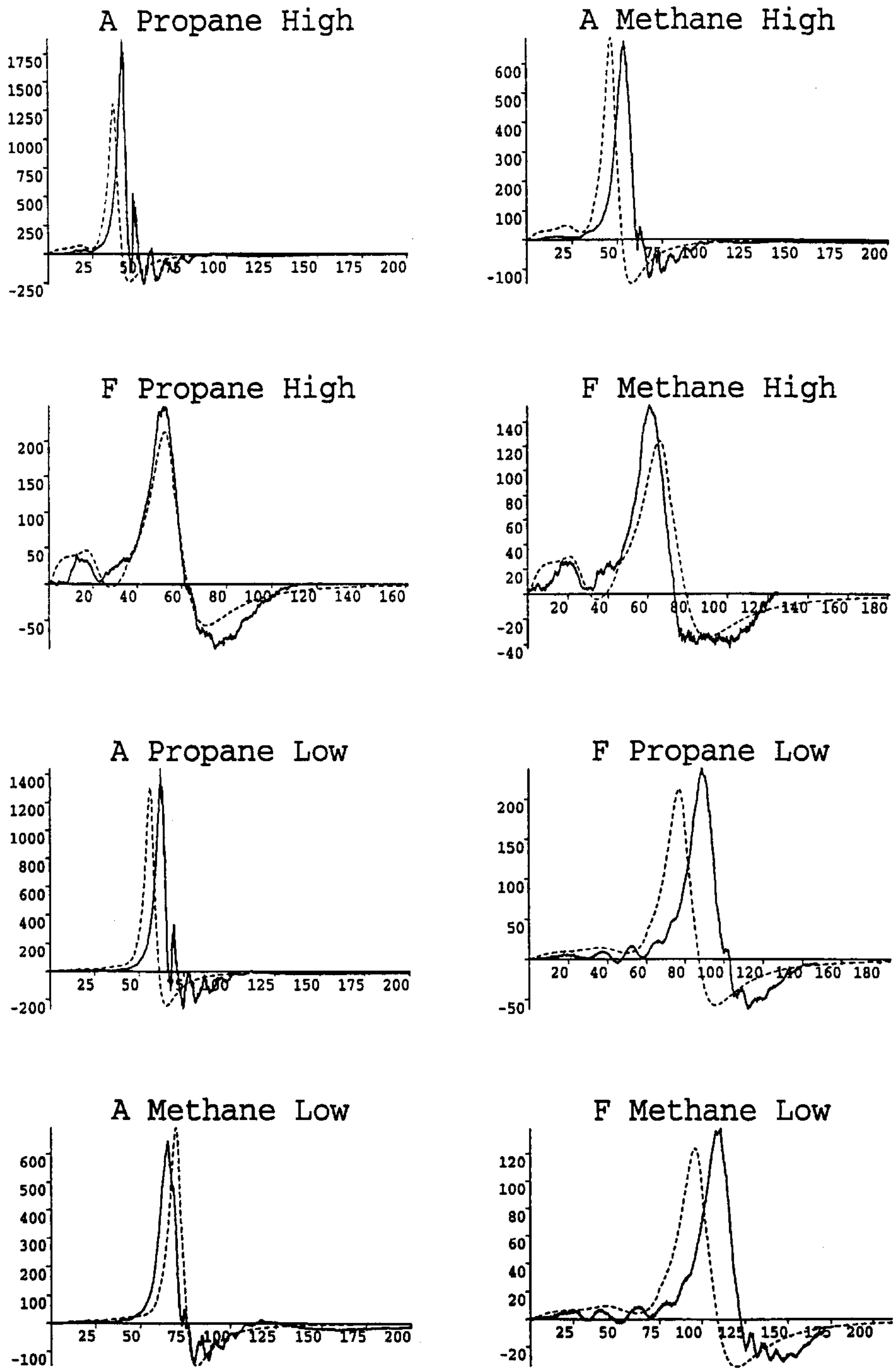
A Propane High
1750
1500
1250
1000
750
500
250
-250
25 50 75 100 125 150 175 200
A Methane High
600
500
400
300
200
100
-100
25 50 75 100 125 150 175 200
F Propane High
200
150
100
50
-50
20 40 60 80 100 120 140 160
F Methane High
140
120
100
80
60
40
20
-20
-40
20 40 60 80 100 120 140 160 180
A Propane Low
1400
1200
1000
800
600
400
200
-200
25 50 75 100 125 150 175 200
F Propane Low
200
150
100
50
-50
20 40 60 80 100 120 140 160 180
A Methane Low
600
500
400
300
200
100
-100
25 50 75 100 125 150 175 200
F Methane Low
120
100
80
60
40
20
-20
25 50 75 100 125 150 175 200

the wave having a pressure, $P = P_\infty + \Delta P$, is defined by the relationship given in Whitham [5] as

$$w = a_0 \sqrt{\left(1 + \frac{\Delta P}{P_\infty}\right) \frac{\left(1 + \frac{\gamma - 1}{2\gamma}\frac{\Delta P}{P_\infty}\right)}{\left(1 + \frac{\gamma + 1}{2\gamma}\frac{\Delta P}{P_\infty}\right)}} + a_0 \frac{\frac{\Delta P}{P_\infty}}{\gamma \sqrt{\left(1 + \frac{\gamma + 1}{2\gamma}\frac{\Delta P}{P_\infty}\right)}} \quad (3)$$

When expanded in powers of $\Delta P / P_\infty$, Eq. (3) provides an expression that is correct to first-order powers for the advection velocity of a weak pressure disturbance, as given in Thompson [6], for example.

This approach has the advantage that the speed of each part of the wave is predicted to increase with increasing pressure. It also does not make any *a priori* assumptions about the shape of the pressure wave originating from the source of the explosion. Therefore, in those cases in which the source overpressure wave does not have a shock front, but has a finite rise time, it predicts that the front face of the wave steepens as it moves away from the source region. Before any shocks are formed, the magnitude of each part of the overpressure wave is assumed to decay in an acoustic manner, so that

$$\frac{\mathrm{d}\Delta P}{\mathrm{d}r} = -\frac{\Delta P}{r} \quad (4)$$

where $r$ is the distance travelled by the wave. The method has been extended in the present work by means of simple numerical relationships of the type suggested by Thompson [6] to follow the progress of the shock front once it has formed. Fig. 7 illustrates how this works in practice. The location of each constituent part of the wave-front in Fig. 7(a) is firstly moved according to Eqs. (3) and (4) to produce the wave forms shown. As no action was taken to prevent it, an overhanging profile is produced, as shown on the right-hand side of Fig. 7(a). However, unlike an overhanging water wave, this multi-valued profile is not produced by a pressure wave in air and a shock-fronted wave is produced instead. Hence, in the application of the method, when this condition is first detected, a correction is applied. The new location of the shock front is defined on a density weighted basis, as sketched in an exaggerated form in Fig. 7(b). It can be shown that under this assumption, the equation governing how fast the shock front moves, $w_s$, is given by

$$w_s = \frac{\int \rho(P) w(P)\,\mathrm{d}P}{\int \rho(P)\,\mathrm{d}P} \quad (5)$$

where $\rho$ denotes the density of the air.

As a result of this, the speed of the shock front is less than the speed corresponding to the maximum of the pressure wave. Therefore, once a leading shock has been produced, its decay rate is faster than the acoustic rate applicable for finite rise time waves.

Fig. 5. Comparison of the observed and predicted overpressures for all the medium scale tests using fuel-air mixtures carried out as part of the EMERGE programme. The letter A or F denotes a different test rig (Table 1) and high or low refers to the level of initial turbulence around the ignition position.

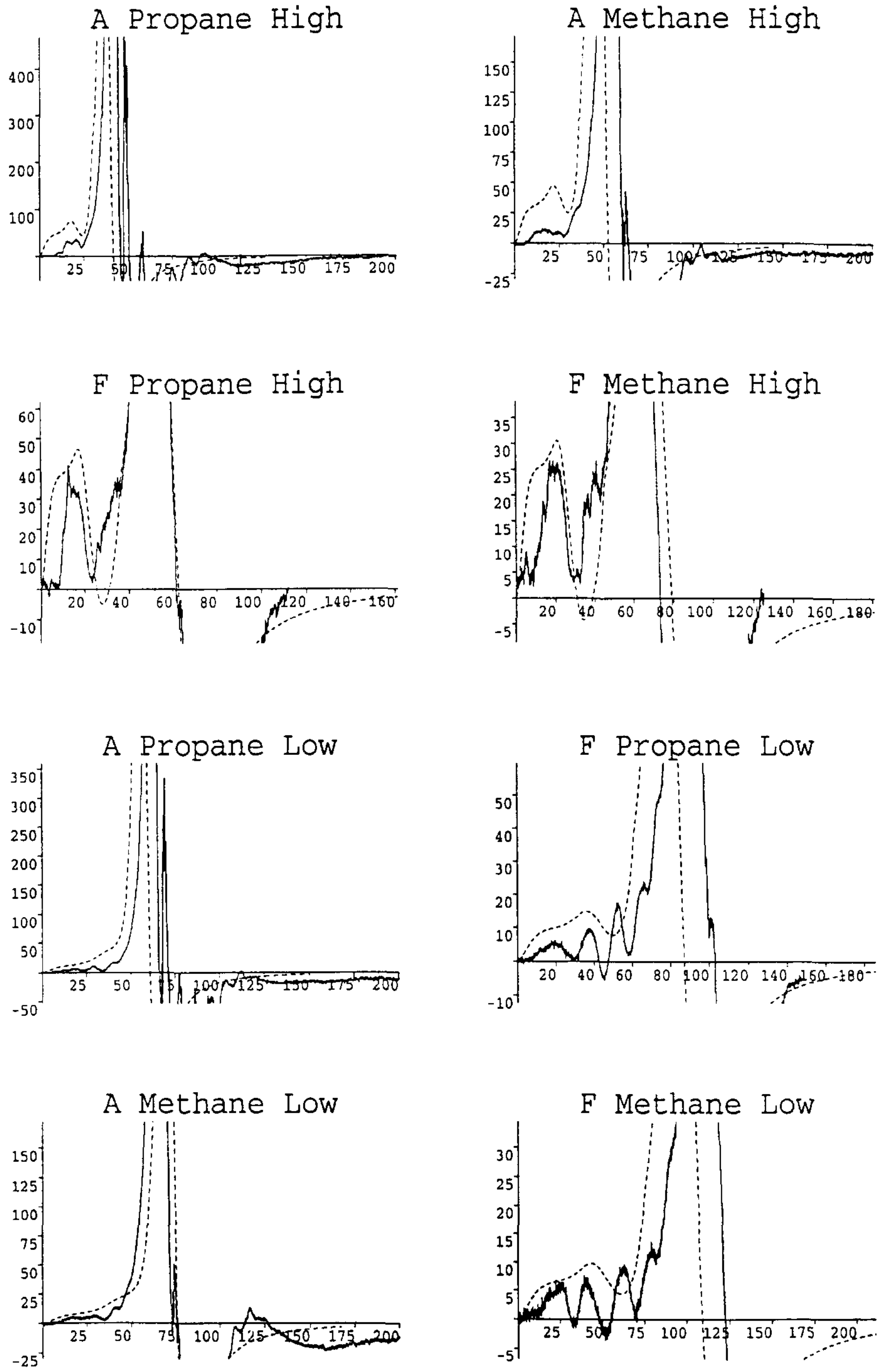


Fig. 6. Detail of Fig. 5 to illustrate the rise in pressure at early times attributed to the initial turbulence field.

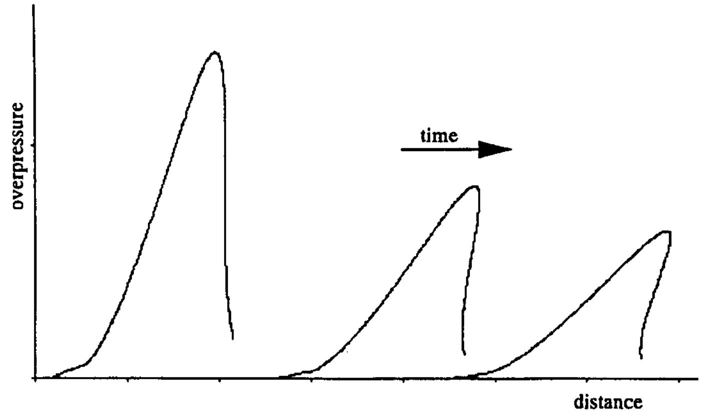


a)

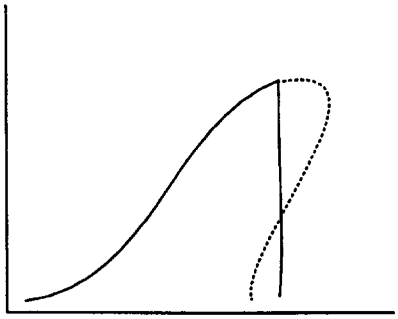

b)

Fig. 7. An illustration of the wave advance method. (a) The results of moving a pressure profile using Eqs. (3) and (4); (b) the method employed to account for shock information.

In the limit of acoustic or weak waves, the above method correctly predicts that a wave will propagate from the source without change of shape. Further, in the other limiting case, Eq. (3) is appropriate for predicting the advance of a shock-fronted wave propagating into still air. This later point is demonstrated by applying the method to predict the propagation of the type of waveform assumed in the application of TNT equivalence methodology (see for example, Baker et al. [7]). Fig. 8 shows that the predictions of the method for a range of cloud volumes are in agreement with the TNT decay curve, as taken from [7]. In the next subsection, experimental data is examined to demonstrate that the method is applicable to the overpressure waves produced in real explosions.

### *3.2. Comparison of the model with data*

The wave propagation model has been verified by comparison with experimental data from the MERGE and EMERGE programmes. External overpressure information

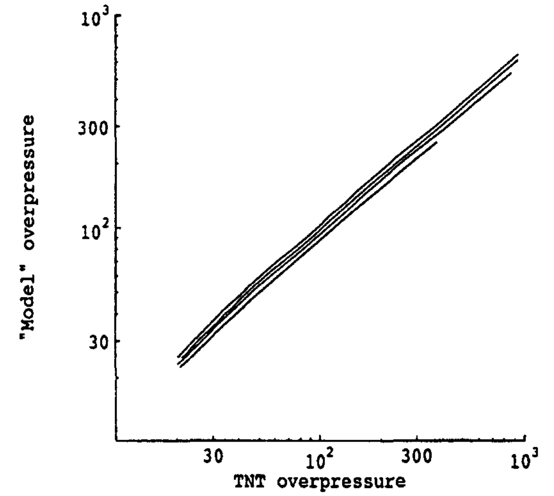


Fig. 8. A comparison of the overpressure as a function of distance predicted by the TNT correlation and by the pressure wave advection model for initial cloud volumes of 10, 100, 1000 and 10000 $m^3$.

recorded 4 m from the centre of the congested region has been used to define the starting conditions for the wave propagation algorithm. The predicted pressure–time profiles at 12 and 48 m from the centre of the congested region were obtained. This demonstrated satisfactory agreement with the experimental values and showed that the correct decay and advection of the waveform is reproduced for a more general shape of overpressure wave. Similar agreement was obtained over the whole of the range of source overpressures produced in the test programme. Profiles recorded in other British Gas experimental test programmes were used to test the model further and satisfactory agreement was obtained.

At present any change in shape of the wave produced by interaction with obstacles has been ignored. If information were required at this level of detail, as with the details of the combustion in the congested region, a more sophisticated approach would be required.

## 4. Prediction of the loading on obstacles

### 4.1. Model formulation

In a recent paper, Catlin et al. [8] proposed a method for determining the loading received by an obstacle subjected to a pressure wave of a general shape. In this method, the magnitude of the transient loading $L(t)$ received by an obstacle is calculated as the sum of three terms as follows:

$$L(t) = \int P(t)\mathbf{n} \cdot \mathbf{e}\, \mathrm{d}S + C_{\mathrm{m}} V \frac{\mathrm{d}(\rho u)}{\mathrm{d}t} + C_{\mathrm{d}} \frac{1}{2} \rho u^2 A_{\mathrm{f}} \tag{6}$$

where **n** is the unit outward normal from the surface of the body, **e** is a unit normal in the direction from the effective centre of the explosion to the centre of the obstacle, $dS$ is an element of surface areas of the obstacle, $C_m$ is an inertial drag coefficient, $V$ is the volume of the obstacle, $C_d$ is a form drag coefficient and $A_f$ is the frontal area of the obstacle, projected on to a plane normal to **e**.

In Eq. (6), the second and third terms, representing the inertial and form drag, are calculated from the flow field ignoring the presence of the obstacle—that is, the "incident" flow from upstream. The first term on the right-hand side of Eq. (6), based on the free pressure field, has been added to account for any differential pressure loading due to gradients in pressure over the length scale of the obstacle. Again, this ignores the changes in the flow and pressure field introduced by the interaction with the obstacle. It is important to account for spatial variations in the incident pressure for shock like wave

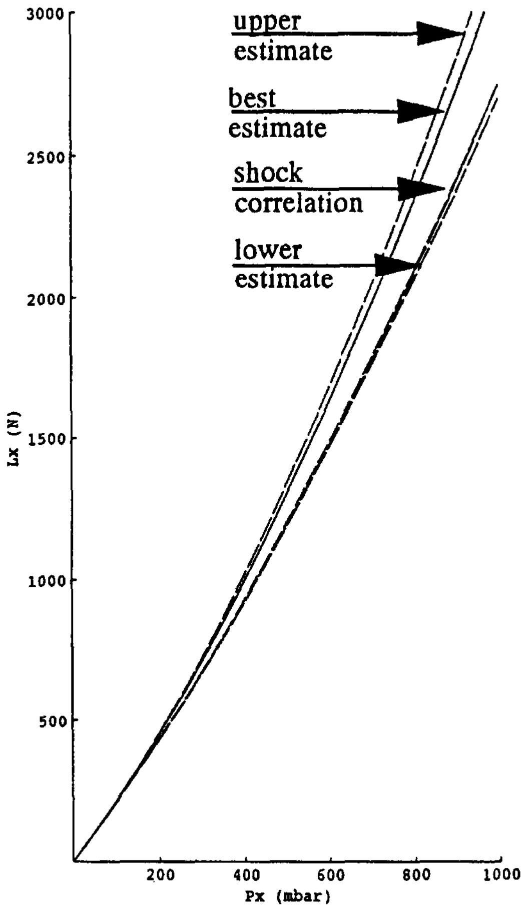


Fig. 9. Predictions for the maximum positive phase load per unit area produced by a simple shock obtained using the correlation in Baker et al. [8] and the general loading model described in Section 4. The "best estimate" is generated using mid-range values of the coefficients appropriate for a vertical cylinder.

forms, as the loading from these waves has a substantial component due to the differential pressure as the wave form travels around the obstacle.

It is possible to determine what the predictions of this approach are like for a steep fronted shock wave of the type assumed in the TNT methodology. Fig. 9 compares the predictions of the loading received on a cylindrical obstacle with the correlations given in Baker et al. [7]. A range of predictions is shown for the model of Catlin et al. [8], corresponding to different values of the drag coefficients. As can be seen, using realistic values for these coefficients, it is possible to encompass within the range of predictions the values that are produced using the TNT method correlations. For the particular case of a steep wave form, provided that a suitable interpretation is made for the inertial term in the model of Catlin et al. [8], it is possible to demonstrate analytically that the two approaches necessarily produce similar results.

### 4.2. Comparison of the model with experimental data

Recent experiments have been carried out by British Gas to investigate the loading received by an upright vertical cylinder, positioned downstream from a gas explosion. Fig. 10 illustrates the experimental situation. The explosion, of known strength and duration, was generated within the semi-confined volume, shown on the left-hand side of Fig. 10. The resulting free field pressure was measured midway between the centre of the open face of the explosion chamber and the centre of the instrumented cylinder and at the various locations shown in Fig. 10. This information was used to define the incident pressure, velocity and density field experienced by the cylinder and Eq. (6) was

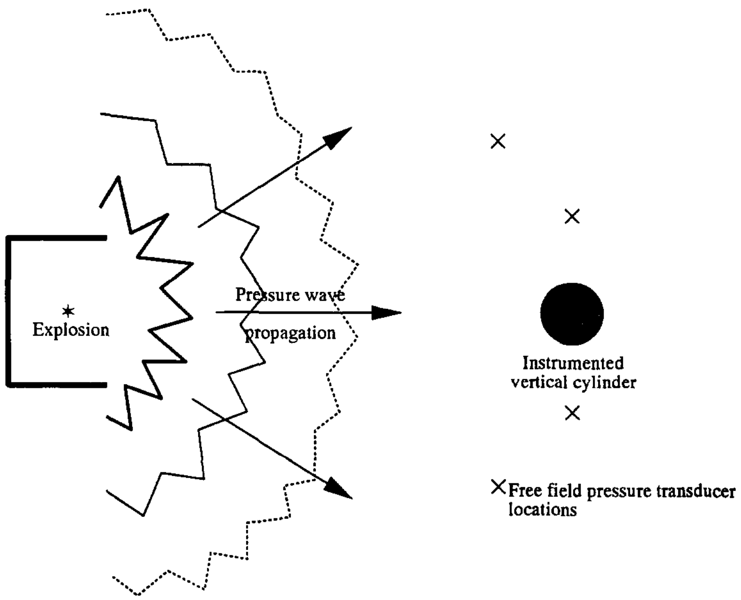


Fig. 10. Sketch of the experimental layout in which the net loading received by a vertical cylinder was measured.

used to predict the total loading received by the cylinder. The cylinder was instrumented in such a way as to allow the loading it receives to be calculated from the measurements in two different ways.

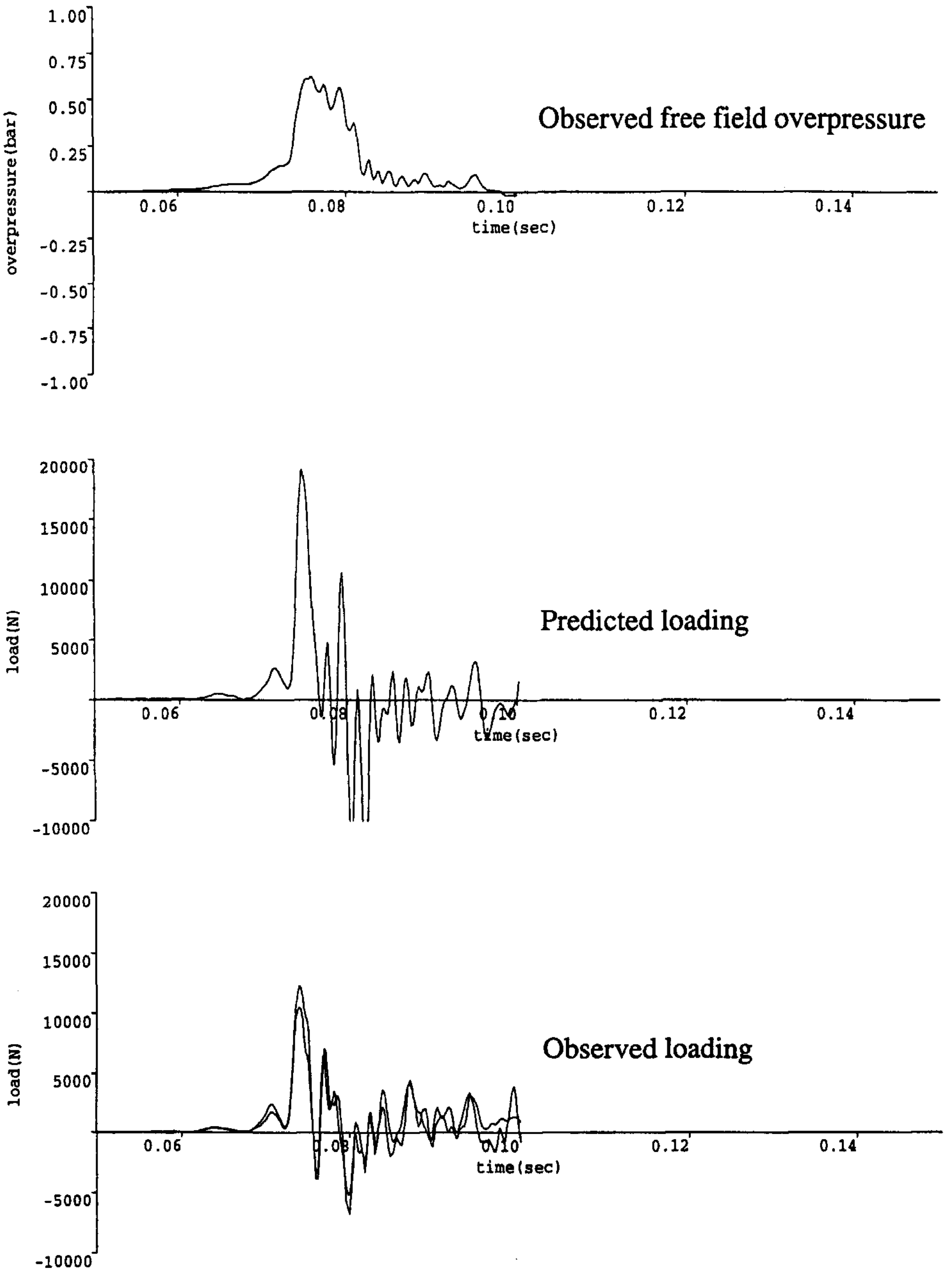


Fig. 11. Comparison of the predicted and observed loading profile for one particular experiment. The observed loading profile was calculated from the measurements using two independent methods.

Fig. 11 illustrates a particular comparison of the predictions of the model with the experimental data. It demonstrates that the method can reproduce the correct transient nature of the received load. Comparisons of the model with all of the experiments in this test series show that the predictions are good for the maximum load, the duration of the first positive phase of the overpressure and the integrated load received during this phase. The equivalent predictions during the first negative phase are not as good, although they lie within a factor of two of the data. It may be that the poorer prediction during the first negative phase points to a weakness in the model, such as the assumption that the first term in Eq. (6) can still be used to infer a differential pressure loading. In practice, also, differences during this phase of the loading may be less significant.

## 5. Discussion and conclusions

In the above sections, a number of separate models have been proposed which can be applied individually to predict component parts of the outcome of a vapour cloud explosion. Furthermore, the methods have been embodied within a computer code in which the output from one stage of the calculation can be used as initial conditions for the next stage. Each of the methods has approximately the same level of sophistication and can be installed on a personal computer with short run times. Representative examples have been given, illustrating how the individual models compare with experimental data for idealized situations. In general, satisfactory agreement has been obtained. The individual models each provide information of about the same quality and complexity.

Comparisons have been given in Section 3 and 4 that demonstrate that if the explosion produced a steep-fronted shock of the type assumed in the TNT methodology, then the resulting predictions for the pressure decay away from the source region and the load received by an obstacle would be broadly similar to the predictions of the TNT method. Therefore, the model would be expected to be at least as useful as TNT-based methods—for example, in situations in which high pressures are generated in the source region and strong shock-like waves are generated at the source.

However, the above approach defines how the pressure generated by an explosion in a compact, congested region varies with the degree of congestion, rather than the less well defined values employed in TNT methods. It also predicts the decay and time history of a more general shape of pressure wave. For example, the steepening of the wave as it travels away from the source is predicted by the model. As Puttock has pointed out [4], in practical cases, it is important to predict the correct behaviour for such waves rather than assume a particular approach, such as acoustic or TNT wave decay, without regard to the source pressure.

In order for this to be a useful approach, the combined method would have to be capable of yielding predictions for a range of source regions containing a distribution of pipe sizes and obstructions within it and for a range of obstacle shapes and sizes receiving the load. In terms of analysing the geometry of a congested region, it is often the case that a CAD package description of regions of plant is available. This includes details of obstructions, pipework and vessels within the region. It is possible to write computer programs to analyse these databases to produce geometric parameters that describe it. For example, an overall volume blockage can be found within a region, as can a suitably defined representative pipe diameter.

For compact (near cube-shaped) regions, these values can then be used within the model defined above to predict the overpressure produced by central ignition of a gas cloud enveloping this region. The sensitivity to alternative definitions of the representative pipe diameter can be investigated and the choice optimized by comparison with appropriate experimental data. Work to-date indicates that, provided the layout of the obstacles does not have a strong directional preference, the use of these average geometric parameters within the model allows a reasonable prediction of the resulting pressure to be made. In particular, it provides a systematic method of differentiating between those regions in which severe overpressures might be produced and those in which more modest overpressure levels are generated.

Finally, it is noted that the loading on any obstacle is calculated in a way that depends on the wave shape as well as its magnitude and duration. This allows the time history of the load to be more accurately predicted, with the potential for an improved analysis of the response of the obstacles to the loading compared with TNT-based methods.

## Acknowledgements

This paper is published by kind permission of British Gas plc. Thanks are due to Clive Catlin and Mike Johnson for their contributions to the work on vapour cloud explosions. Some of the work contained in Section 2 was carried out as part of project EMERGE, with financial support from the European Commission through the STEP programme under Directorate-General XII (contract EV5V-CT93-0274), and this support is gratefully acknowledged.

## References

[1] R.P. Cleaver and C.G. Robinson, An analysis of the mechanisms of overpressure generation in vapour cloud explosions, *J. Hazard. Mater.*, *45* (1996) 27–44.
[2] W.P.M. Mercx, Modelling and experimental research into gas explosions. Overall final report of the MERGE project, *CEC contract STEP-CT-0111(SSMA)*, 1993.
[3] A.C. van den Berg, The multi-energy method: a framework for vapour cloud explosion blast prediction, *J. Hazard. Materi.*, *12* (1985) 1–10.
[4] J.S. Puttock, Fuel gas explosion guidelines—further development, in *Second European Conf. Major Hazards On- and Off-shore, Manchester, 24–26 October*, 1995.
[5] G.B. Whitham, *Linear and Nonlinear Waves*, Wiley, New York, 1974.
[6] P.A. Thompson, *Compressible Fluid Dynamics*, McGraw-Hill, New York, 1972.
[7] W.E. Baker, P.A. Cox, P.S. Westine, J.J. Kulesz and R.A. Strehlow, *Explosion Hazards and Evaluation*, Elsevier, Amsterdam, 1983.
[8] C.A. Catlin, M. Mishein and B.M. Younger, The blast loading imparted to a cylinder by venting of a confined explosion, in *Offshore Structural Design against Extreme Loads, 3–4 November, 1993, London.* (Published in ERA Report 93-0843, January 1994.)